ELSEVIER

Catalysis Today 59 (2000) 231–240

CATALYSIS TODAY

www.elsevier.com/locate/cattod

Group VI transition metal carbides as alternatives in the hydrodechlorination of chlorofluorocarbons

L. Delannoy, J.-M. Giraudon*, P. Granger, L. Leclercq, G. Leclercq

Laboratoire de Catalyse de Lille, UPRESA CNRS 8010, Université des Sciences et Technologies de Lille, 59650 Villeneuve d'Ascq Cedex, France

Abstract

The synthesis of transition metal carbides of tungsten and molybdenum has been carried out via temperature programmed reactions (TPRs) of metal oxides or passivated nitrides. Their specific chloropentafluoroethane conversion rates were at best one order of magnitude less than that of a reference Pd based catalyst. The intrinsic rates range from 4.7 to 14.7 nmol m^{-2} s^{-1} and decrease as follows: Mo_2C>WC>W_2C≈WC_{1-x}>MoC_{1-x}. The group VI carbide samples catalyse hydrodehalogenation and dehydrofluorination. WC appears to be as selective towards pentafluoroethane (HFC-125) as the Pd based catalyst. Then the selectivity decreases in the following sequence: W_2C>Mo_2C>WC_{1-x}>MoC_{1-x}. All the carbide catalysts deactivate at the early stages of the reaction. Based on the XPS results and the product distribution of the reaction, the deactivation has been mainly attributed to a site blocking phenomenon due to a strong deposit of polymeric carbon and of hydrofluorocarbon polymers. Polymerisation of detected unsaturated compounds take place on acidic sites probably generated by fluoride and/or chloride in the course of the reaction.

Keywords: Group VI carbide catalysts; Hydrochlorination; Chlorofluorocarbons; Deactivation

1. Introduction

The synthesis of substitutes of fully halogenated chlorofluorocarbons (CFCs) is an important task from an industrial viewpoint since they behave like ozone killers [1] and contribute to the greenhouse effect [2]. So, destruction of such species has been envisioned since their production and uses have been phased out under international agreements at the Montreal Protocol [3]. Presently, several options for their replacement are available. Among them, the conversion of CFCs into valuable compounds like hydrofluorocarbons (HFCs) seems to be an attractive route [4]. For instance HFCs exhibit similar properties as CFCs without being harmful towards ozone since they readily decompose in the lower atmosphere.

Although since the early 1960s, palladium has been the preferred catalyst for the hydrogenolysis of carbon–chlorine bond, transition metal carbides, especially of group VI, which are also well known to show interesting behaviours in various reactions catalysed by noble metals [5] could a priori promote such a type of reaction.

Indeed Morikawa et al. [6] have reported in a patent that tungsten and molybdenum carbides can be catalytic active species. As exemplified, a catalyst composed of WC granules mixed with $Al(OH)_3$ and spread on Al_2O_3 honeycomb support was active for the dehalogenation of the haloethane CFC-114a.

* Corresponding author. Tel.: +33-3-20-45-40; fax: +33-3-20-65-61.
E-mail address: jean-marc.giraudon@univ-lille1.fr (J.-M. Giraudon)

0920-5861/00/$ – see front matter
PII: S0920-5861(00)00289-3

Two other studies on hydrodechlorination of CFCs over such materials have confirmed such a trend. It has been found that highly dispersed oxycarbides $W_2(C, O)$ exhibit a catalytic activity for the hydrodehalogenation of dichlorodifluoromethane [7]. These materials have been prepared on a passive SiC-coated alumina by first making a transition metal salt, such as chloride, to react with a carbon–nitrogen acyclic compound deficient in carbon as guanidine and then pyrolysing the resulting composition at a temperature of 775°C. The best results have been obtained at a hydrogen to CCl_2F_2 (CFC-12) ratio of $\frac{1}{4}$ leading to a selectivity towards CH_2F_2 (HFC-32) up to 95.1% at 350°C after 8.5 h time-on-stream. Various supported and unsupported carbide materials have also been studied for their activity in the same reaction as above [8]. Whatever is the catalyst under consideration, it shows a selectivity towards the formation of HFC-32 of 100%. If the turnover numbers of the supported carbides were found to be higher than the unsupported ones, they deactivated quickly with time.

Thus, because of the lack of fundamental information on the hydrodechlorination of chlorofluoroalkanes over metal carbide materials, the catalytic performances of bulk tungsten and molybdenum carbides have been investigated in the hydrogenolysis of the chloropentafluoroethane (CF_3CF_2Cl, CFC-115). The desired product of the reaction CF_3CF_2H (HFC-125) is believed to be a promising substitute of R-502, which is an azeotropic blend of $CHClF_2$ and CF_3CF_2Cl.

This study will be focused on the influence of the metal atom and of the lattice structure of the catalysts upon the catalytic properties. The catalytic results will also be compared with those of a reference Pd/C.

2. Experimental

2.1. Synthesis procedure

The preparation of the carbides was carried out via temperature programmed carburisation of bulk metal oxides (MoO_3 — 99.95%, Fluka and WO_3 — 99.95%, Fluka) or passivated nitrides. The nitrides were synthesised by temperature programmed reactions (TPRs) of MO_3 (M=Mo, W) with NH_3 (99.96%, Alphagas). The molybdenum sample was rapidly heated from room temperature to 345°C (465°C for W) for about 0.5 h. Then it was heated following two linear heating segments. The temperature was first raised from 345 to 450°C at 36°C h^{-1} and then from 450 to 750°C where the final temperature was kept for 1 h. For tungsten, the powder was heated from 465 to 750°C and held at the final temperature for 6 h. The molar hourly space velocity was 90 h^{-1} (Mo) and 96 h^{-1} (W). After cooling to room temperature the samples were passivated in a 2% O_2/N_2 for 5 h (2 l h^{-1}).

The method of carburisation consisted of contacting a carbiding mixture composed of 10 or 20 vol.% CH_4 (99.995%, Air Liquide) in hydrogen (99.995%, Air Liquide) over the oxides or the passivated nitrides subsequently reduced under H_2 at 450°C for Mo_2N or 500°C for W_2N for 10 h. The temperature was raised in a progressive manner (1°C min^{-1}) to the final temperature θ_{fin} and held at this level till the reaction was completed. Such experimental conditions used for the carburisation were summarised in Table 1. They led practically all the samples to a minimisation of excess polymeric carbon deposit produced by the decomposition of methane during carburisation. Thus, no activation treatment was undertaken except in the case

Table 1
Experimental conditions for the preparation of group VI transition metal carbides

Catalyst	Precursor	Carburisation 10* or 20 vol.% CH_4/H_2			Carbide phase	Structure[a]
		Flow (cm^3 min^{-1} g^{-1})	θ_{fin} (°C)	Isotherm. (h)		
WC	WO_3	110	800	8	α-WC	hex
W_2C	WO_3	110	630	8	α-W_2C	h.c.p.
Mo_2C*	MoO_3	110	700	5	β-Mo_2C	h.c.p.
WC_{1-x}	W_2N	167	750	0.5	β-WC_{1-x}	f.c.c.
MoC_{1-x}	Mo_2N	167	700	3	α-MoC_{1-x}	f.c.c.

[a] hex: simple hexagonal; h.c.p.: hexagonal close-packed; f.c.c.: face-centred cubic.

of WC, which was submitted to a 1% CH_4/H_2 flow at 800°C for 6 h. All the samples were finally passivated with a 2% O_2/N_2 mixture at room temperature before being characterised.

2.2. Characterisation

X-ray diffraction (XRD) measurements were conducted in a diffractometer SIEMENS D5000 using Cu Kα radiation (λ=0.15418 nm). XRD patterns were assigned with the JCPDS database. The average size of the crystallite was calculated from the Scherrer equation $D_c=K\lambda/B\cos\theta$ where K is a constant (taken here to be 0.9), B the corrected peak width and θ the Bragg angle of the peak.

X-ray photoelectron spectroscopy (XPS) was performed on a Leybold-Haraeus LHS10 spectrometer equipped with an Al anode ($h\nu$=1486.6 eV). The binding energies (BEs) were referenced to the binding energy level of O 1s at 531 eV.

The specific surface areas were measured with a sorptometer Quantasorb Jr. using the single point BET surface area determination. The average particle size was estimated from the derived equation $D_p=6/\rho S_g$, where ρ is the bulk carbide density and S_g is the specific surface area assuming that the particles were spherical and/or cubic.

2.3. Catalytic testings

The hydrogenolysis of CFC-115 was carried out in a stainless steel fixed bed flow reactor (10 mm i.d.–12 mm o.d.) at atmospheric pressure. The experimental set-up was described in Fig. 1. All catalytic experiments were performed on carbide catalysts prepared in situ according to the following experimental procedure. About 1 g of the catalyst was placed in the reactor. After synthesis, the samples were cooled in the carbiding mixture to the reaction temperature at 350°C. H_2/CF_3CF_2Cl molar ratio was 2. The total flow rate was 2.5 l h^{-1} (corresponding to a volumetric space velocity of about 4000 h^{-1}). The reacting mixture was then allowed to pass over the catalyst at atmospheric pressure. The 1 wt.% Pd commercial catalyst supported on activated charcoal (Accros Chemicals) was activated in H_2 for 10 h at 350°C before the catalytic run. The outlet gas mixture was analysed by a chromatograph Shimadzu GC-9A equipped with a thermal conductivity detector after passing, respectively, through a water bath (to trap HCl and HF formed during the reaction) and a filter (drierite). The reactant and products were separated on a plot fused silica (50 m×0.53 mm) column (Chrompack). All the quantified gaseous components were previously identified with a mass spectrometer Omnistar GSD 3000 from Balzers.

3. Results

3.1. Synthesis and characterisation of the carbide catalysts

XRD patterns of the passivated catalysts freshly prepared are presented in Fig. 2. Peak positions are clearly consistent with the desired crystallographic phases listed in Table 1. So the materials are phase-pure except for the MC_{1-x} samples, where a small contribution of α-WC and β-Mo_2C is detected.

XPS results are reported in Table 2. The BEs of the W $4f_{7/2}$ and Mo $3d_{5/2}$ photoelectron peaks, respectively, at 32.2 and 228.8 eV are in good agreement with a metal carbide phase [9,10]. The C 1s spectrum in Fig. 3 exhibits two main components, the lower binding energy one at ca. 283.3 eV characterises a carbon linked to tungsten, while the contribution at 285 eV is ascribed to polymeric carbon [9]. Thus, the carbide is clean as long as the intensity of the low binding energy component is high. So a lower carbon contamination on WC, W_2C and Mo_2C is expected than on MoC_{1-x} and WC_{1-x} samples. This is indeed reflected quantitatively by the values of the $C_{carbide}/C_{(carbide+polymeric)}$ atomic ratio. Noteworthy here is the substantial amount of polymeric carbon retained by the WC_{1-x} solid. Besides XPS, metal carbide stoichiometry has been determined and shows that the $(C/W)_{carbide}$ ratio is approximately the same for the h.c.p. and f.c.c. phases, i.e. α-W_2C and WC_{1-x} considering the margin of error.

The resulting BET surface areas of the carbide catalysts, ranging from 13.5 to 96 $m^2\,g^{-1}$, are noticeably higher than those of the oxide precursors (ca. 3 $m^2\,g^{-1}$). For the medium surface area catalysts, the crystallites are much smaller than the particles suggesting the formation of polycrystalline particles,

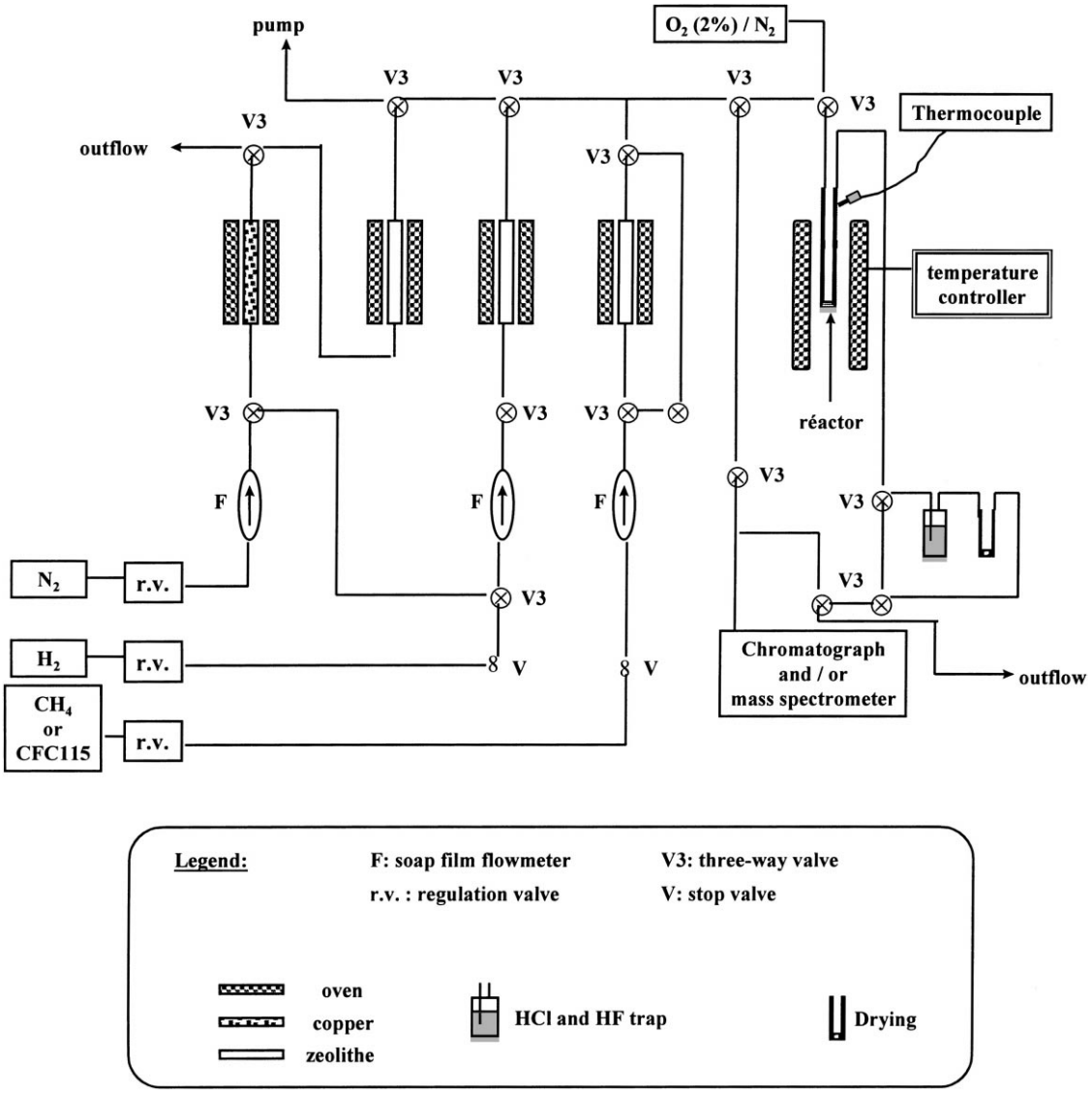

Fig. 1. Experimental catalytic set-up.

whereas for the higher surface area catalysts, the crystallite and particle sizes are similar (Table 3).

3.2. Catalytic properties

The evolution of (τ_n/τ_1) at 350°C (where τ_n is the conversion after n hours) with time-on-stream is illustrated in Fig. 4(a) and (b). Whatever is the carbide catalyst under consideration, deactivation occurs at the early stages of the reaction, a pseudo-stationary state being reached after ca. 6 h on stream. In contrast, the Pd catalyst deactivates more slowly with time. Clearly the initial deactivation operates more readily on WC_{1-x} than on W_2C and WC. Such tendency is also observable on molybdenum catalysts, Mo_2C being more resistant to deactivation than MoC_{1-x}.

In Table 4 the conversion, specific and intrinsic rates after 1 h of test run **(**which is the time required for the

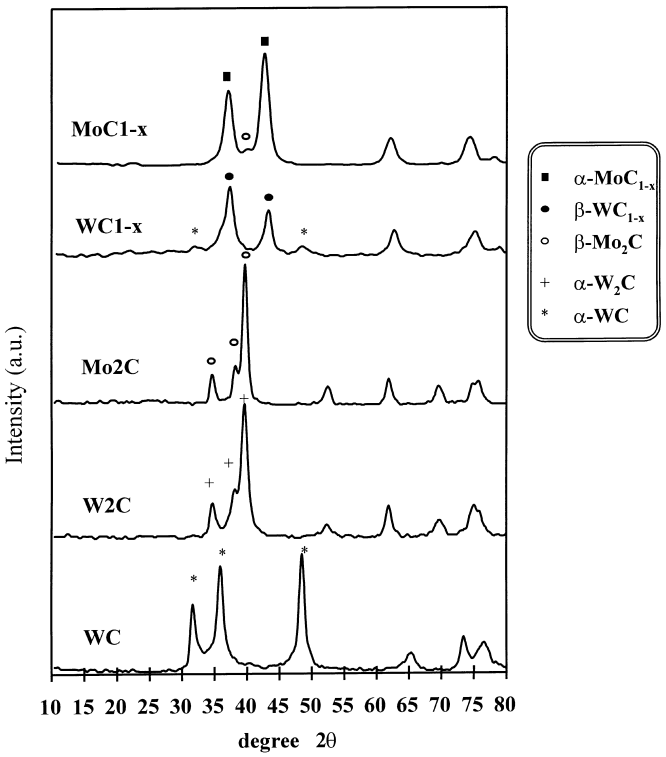

Fig. 2. X-ray diffraction patterns of the carbide catalysts freshly prepared. Peaks attributed to the crystalline phases in the right panel are indicated by the appropriate symbol.

stabilisation of the system) and at pseudo-stationary state are given. As observed, the specific reaction rates of the carbides are lower than that of the palladium based catalyst.

Among carbides, the MC_{1-x} samples are the most active catalysts at initial stages of the reaction; this can be readily explained owing to their higher BET surface areas as reflected by the values of the activity expressed in nmol m^{-2} s^{-1}. Let us notice that the residual steady state specific activity of the most active carbide catalyst is one order of magnitude lower than that of the reference Pd/C catalyst. Intrinsic activities of the carbides at the pseudo-stationary state range from 4.7 to 14.7 nmol m^{-2} s^{-1} at 350°C and decrease as follows: Mo_2C>WC>W_2C≈WC_{1-x}>MoC_{1-x}.

Product distribution of the different carbide catalysts as the one of the Pd/C at steady state (after about 13 h on stream) is given in Figs. 5 and 6. Considering the low pseudo-stationary state conversion on all the carbide catalysts (about 1%), the discrepancies

Table 2
XPS data of the fresh carbide catalysts

Catalyst	Photopeak	Binding energy (eV)	$C_{carbide}/C_{(carbide+polymeric)}$	$C_{carbide}/M_{carbide}$
WC	W $4f_{7/2}$	32.2	0.71	1.06
W_2C	W $4f_{7/2}$	32.2	0.77	0.66
Mo_2C	Mo $3d_{5/2}$	228.8	0.74	0.63
WC_{1-x}	W $4f_{7/2}$	32.3	0.18	0.55
MoC_{1-x}	Mo $3d_{5/2}$	228.8	0.52	0.78

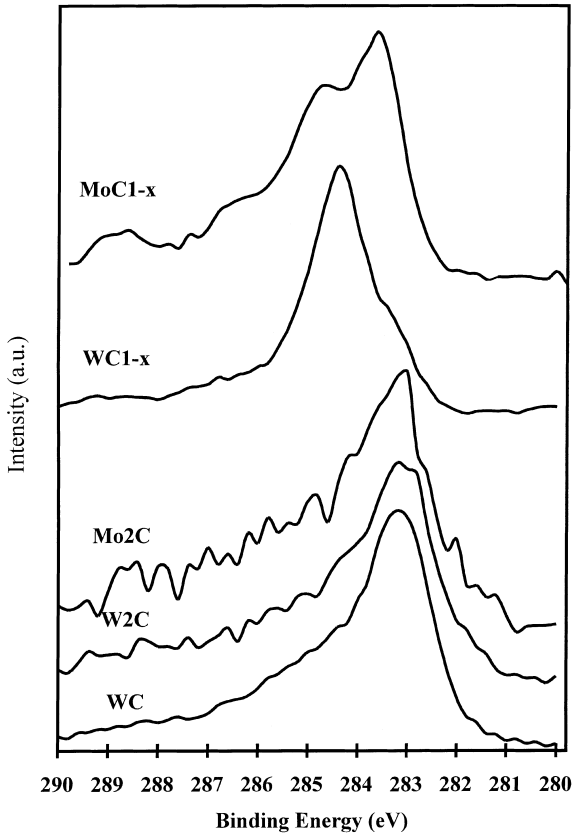

Fig. 3. C 1s XPS spectra of the group VI metal carbide freshly prepared.

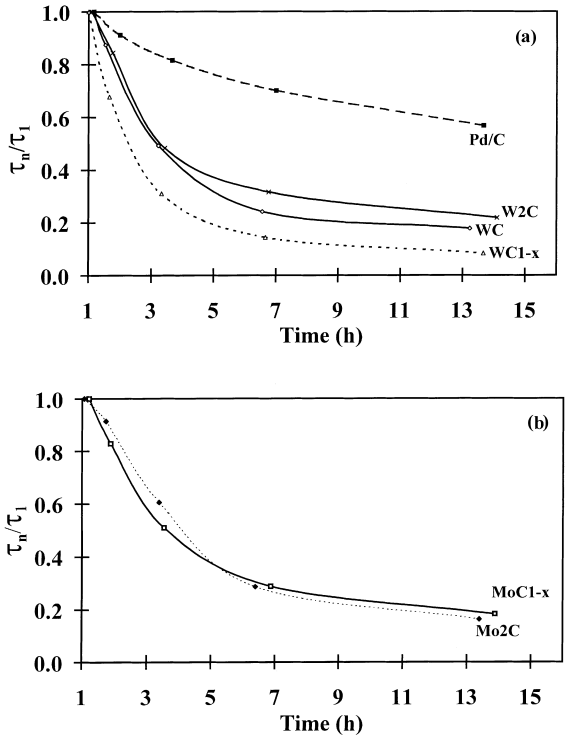

Fig. 4. (a, b) Time-on-stream behaviour of the catalysts in the reaction of hydrodechlorination of CF_3CFCl_2 at 350°C (τ_n is the conversion after n hours, H_2/CFC=2).

between the product distributions are not ascribed here to different conversion levels. As far as the selectivity towards pentafluoroethane (HFC-125) is concerned, several observations can be noted. Firstly, WC appears as highly selective as the Pd based catalyst; these two samples being more selective than the other related tungsten and molybdenum based catalysts. Secondly, among the tungsten carbide based catalysts, selectivity decreases owing to the sequence: WC>W_2C>WC_{1-x}. Thirdly, it appears that irrespective of the nature of the metal, the hexagonal close packed phase is more selective towards pentafluoroethane than the face-centred cubic one.

Table 3
Physico-chemical characterisation of the fresh and spent catalysts

Catalyst	Fresh catalyst			Spent catalyst		
	Specific surface area ($m^2\ g^{-1}$)	Crystallite size (nm)	Particle size (nm)	Specific surface area ($m^2\ g^{-1}$)	Crystallite size (nm)	Particle size (nm)
WC	15	7.9	25.5	14	7.8	27.3
W_2C	19	8.4	18.4	18	9.2	19.4
Mo_2C	13.5	11.1	48.9	13.5	11.2	48.9
WC_{1-x}	52	7.4	6.7	42	7.8	8.3
MoC_{1-x}	96	7.9	6.6	58	8.3	10.9

Now let us examine the by-product distribution in Fig. 6. They can be arranged in three categories: (1) alkanes (essentially CH_4 and C_2H_6 and to a minor extent C_3H_8); (2) unsaturated compounds (essentially C_2H_4 and to a minor extent $C_2H_2F_2$ and C_2F_4); (3) C_2 defluorinated compounds (CF_3CFH_2 (HFC-134a) and CF_3CH_3 (HFC-143a)). As observed, Pd produces defluorinated compounds, whereas by-products on carbides are essentially alkanes and unsaturated compounds. It is also noteworthy that the crystallographic structure of carbides influences the selectivity towards the formation of unsaturated compounds, which remarkably increases according to the sequence hex<h.c.p.<f.c.c., it is also noticeable that the W carbide based catalysts are more hydrogenating catalysts than the Mo ones as shown by the comparison of the C_2H_6/C_2H_4 ratios.

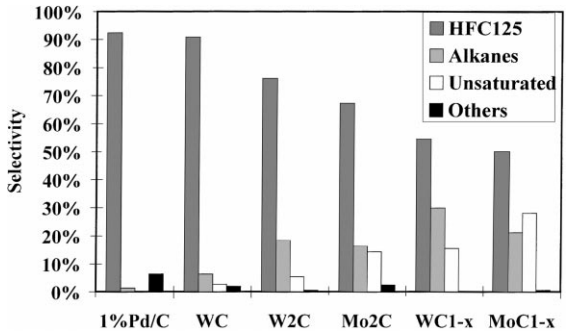

Fig. 5. Product distribution by family at pseudo-stationary state for the Pd/C and group VI transition metal catalysts at 350°C.

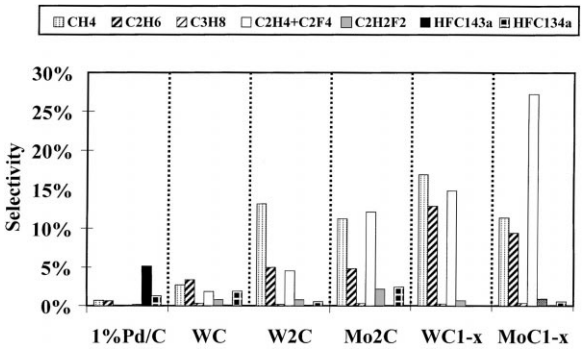

Fig. 6. By-product distribution at pseudo-stationary state for the Pd/C and group VI transition metal carbides at 350°C.

3.3. Characterisation of the spent catalysts

The spent catalysts have been characterised in order to have an insight into the deactivation process. Notice that they were prior passivated according to the procedure described earlier. The examination of the XRD patterns does not show bulk reconstruction as each catalyst retains its initial carbide phase. Additionally the crystallite size does not vary significantly (Table 3). On the other hand, the BET surface areas decrease for the MC_{1-x} samples, whereas no significant variations are observed for the other samples.

The examination of both the chemical state and surface composition of carbon and halogens by XPS are more relevant here (Table 5). An increase in the carbon content is observed after reaction. Additionally one detects a significant amount of fluorine (ca. 20%), and chlorine at a low level (about 1%). As illustrated in Fig. 7(a), the C 1s signal of a WC catalyst shows significant changes after reaction. One notes an additional peak at 284.9 eV due to an excess of polymeric carbon deposit at the surface and the appearance of a tail

Table 4
Conversion, specific rate and activity of the catalysts at 350°C, with H_2/CFC115=2, and a volumetric space velocity of 4000 h^{-1}

Catalyst	Conversion (%)	Specific rate (μmol s^{-1} g^{-1})		Activity (nmol m^{-2} s^{-1})	
		After 1 h	Stationary state	After 1 h	Stationary state
1% Pd/C	26.0	4.9	4.1	–	–
WC	6.3	0.5	0.1	32.0	9
W_2C	4.9	0.4	0.1	19.0	7
Mo_2C	7.5	0.5	0.2	39.0	15
WC_{1-x}	20.0	1.5	0.3	29.0	6
MoC_{1-x}	13.0	1.3	0.5	13.0	5

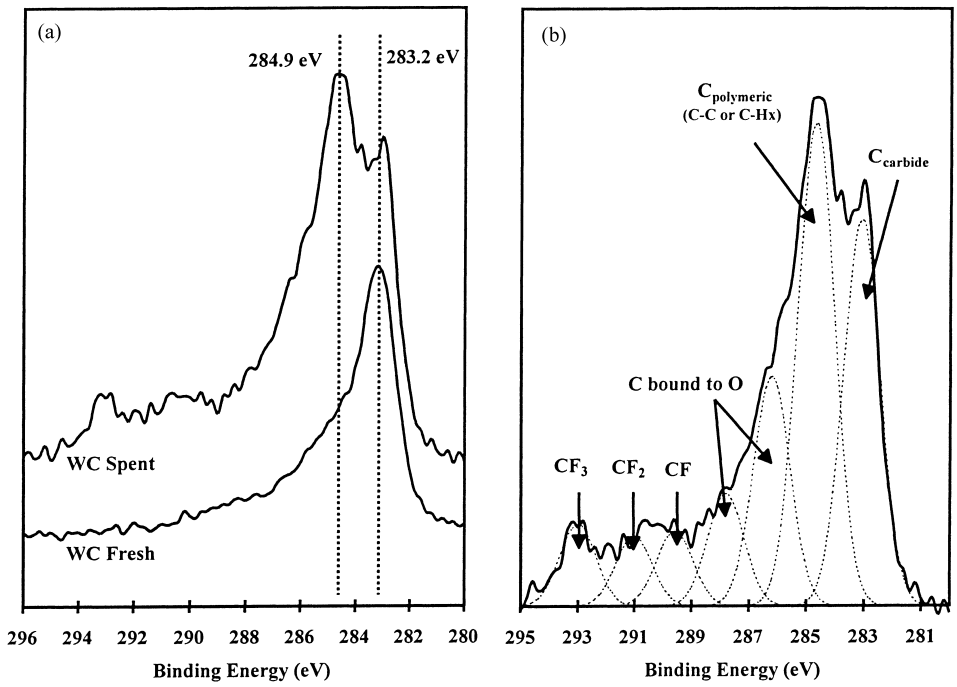

Fig. 7. (a) C 1s XPS spectra of the fresh and spent WC catalyst. (b) Decomposition of the C 1s spectrum of the spent WC catalyst.

in the envelop at higher BEs which indicates different carbon–fluorine species. As shown in Fig. 7(b), such contributions on the C 1s photoelectron peak could be assigned to various organic fluorocarbon species (CF at 289 eV, CF_2 at 291 eV and CF_3 at 293.4 eV [11]). The symmetrical F 1s signal at 688.8±0.2 eV corresponding to an organic fluorine [11] is in agreement with this previous assignment (Fig. 8(a)). A low intensity broad peak of Cl 2p (FWHM ≈5.5 eV) is also observed at 200±0.3 eV (Fig. 8(b)).

Table 5
Surface atomic composition of carbide catalysts estimated from XPS data

Catalyst	C (at.%)		F (at.%)	Cl (at.%)	F/C_{total}
	Fresh	Spent			
WC	32.3	48	22.6	0.8	0.47
W_2C	15.5	49.7	17.4	1.1	0.35
Mo_2C	16.4	49.1	18.4	1.2	0.46
WC_{1-x}	42	55.9	17.1	1.9	0.41
MoC_{1-x}	27.4	60.6	19	1.6	0.32

4. Discussion

This study deals with the catalytic performances of tungsten and molybdenum carbides in the hydrodechlorination of chloropentafluoroethane to be compared with those of a Pd based catalyst commonly used for such a reaction [12]. The most prominent observations are closely related to significant changes in the selectivity and stability of carbide catalysts, which strongly differ from those observed on Pd/C.

As indicated by the examination of the product distribution on carbides, such materials seem to exhibit a bifunctional behaviour towards the transformation of CFC-115 enlightened by various products obtained from C–X (X=F, Cl) bond cleavage (mainly HFC-125) and those resulting formally from dehydrofluorination reactions (C_2H_4, C_2F_4 and $C_2H_2F_2$). Accordingly, carbide catalysts exhibit both hydrogenolysis and dehydrofluorination properties contrarily to palladium since its selectivity behaviour mainly reflects hydrogenolysis properties. As hydrogenolysis reflects the pseudo-metallic properties, by contrast, dehydrofluorination would involve acidic

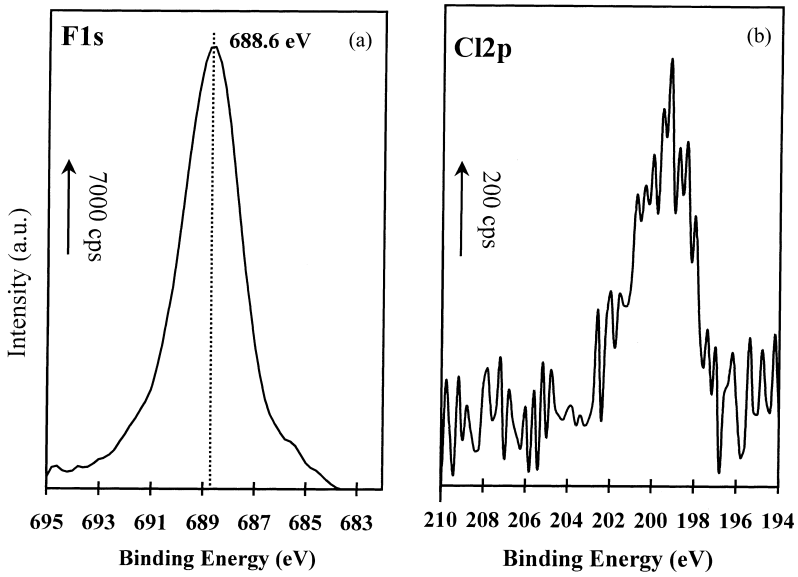

Fig. 8. (a) F 1s XPS spectrum of the spent WC catalyst. (b) Cl 2p XPS spectrum of the spent WC catalyst.

sites [13]. It is also worthwhile to note that the balance between hydrogenolysis and dehydrofluorination depends on the nature of the carbide lattice structure. Clearly the values for the unsaturated/HFC-125 ratio are much higher for the f.c.c. MC_{1-x} phase than for the related hexagonal ones associated to α-WC, α-W_2C and β-Mo_2C.

More relevant is the high selectivity of WC towards HFC-125 (92%), which is quite similar as that of Pd/C which could give to this former catalyst a potential interest according to an improvement of both its activity and stability. Such a requirement implies a better understanding of the functioning mode of carbide catalysts since it is well established that the control of the surface composition of the carbide catalysts is difficult to handle due to their high sensibility to traces of oxygen when they get rid of polymeric carbon. The role of oxygen is ambiguous because, as carbon, oxygen can diffuse into the interstices of the carbide lattice to give an oxycarbide having a lattice structure very similar to the carbide one. So, despite our caution to avoid oxygen contamination, the presence of very low amounts of oxygen in the course of the reaction cannot be ruled out here.

One important point for discussion in this study is the strong deactivation of the different carbide catalysts at the early stages of the reaction in contrast to the palladium based catalyst. Bulk and surface characterisations suggest that the deactivation is not related to either phase transformation or sintering reactions leading to structural modifications. On the other hand, the significant amount of polymeric carbon and of HFC species observed after reaction on the deactivated catalysts seems to be in agreement with a deactivation by site blocking. These strongly adsorbed species could be the result of the polymerisation of detected unsaturated compounds which usually takes place on strong acidic sites [13]. Such a mode of deactivation can explain the fastest deactivation of the MC_{1-x} catalysts since they are probably more microporous than the other ones although no clear apparent correlation appears between the surface areas and the pore size distribution [14].

An important question which arises here is the origin of such an acidity on these materials. Strictly speaking, the intrinsic acidity of metal carbides could be related to the partial ionicity of the $M^{\delta+}$–$C^{\delta-}$ bond. However, we believe that the extent of such an acidity cannot completely explain the changes in product distribution of Mo and W carbide based catalysts, particularly towards the formation of unsaturated compounds. On the other hand, such a change in the

selectivities could be induced by an alteration of the surface properties of carbide catalysts due to a subsequent incorporation of residual oxygen and/or to the adsorption of hydrogen fluoride or chloride during the reaction. A previous investigation of the hydrogenolysis of ethane over WC, samples considering a ratio C_2H_6/H_2 of $\frac{1}{2}$ does not afford significant polymeric carbon deposit after 24 h on stream. According to this previous observation, we believe that the deactivation is mainly related to an induced acidity due to the occurrence of surface fluoride and chloride species even though XPS results do not formally indicate a fluorination and/or chlorination of the carbidic surface. It is noticeable that a previous investigation of Oyama [8] agrees with this point of view.

5. Conclusion

To conclude, α-WC appears highly selective towards the hydrogenolysis of the chlorine–carbon bond, as selective as our Pd reference, in the case of CF_3CF_2Cl as reactant. However, all the carbide catalysts show a rapid deactivation in the early stages of the reaction. This deactivation is strongly believed to occur from acidic sites which generate unsaturated compounds which are able to polymerise to give an HFC polymer responsible for the deactivation process.

Acknowledgements

Support of this work by the MESR is gratefully acknowledged. We also thank Mrs. Moineau for XPS measurements and Mrs. Burylo for performing the X-ray diffraction studies.

References

[1] M.J. Molina, F.S. Rowland, Nature 249 (1974) 810.
[2] Executive Summary of the Scientific Assessment of Ozone Depletion, 1991.
[3] UNEP, Montreal Protocol on Substances that Deplete the Ozone Layer, Final Act, 1987.
[4] L.E. Manzer, V.N.M. Rao, Adv. Catal. 39 (1993) 329.
[5] S.T. Oyama, Catal. Today 15 (1992) 179.
[6] S. Morikawa, M. Yoshitake, S. Tatematsu, Japan Patent No. 319,442 (1989).
[7] F.G. Sherif, US Patent No. 5,426,252 (1995).
[8] B. Dhandapani, S.T. Oyama, Catal. Lett. 35 (1995) 353.
[9] L. Leclercq, M. Provost, J. Grimblot, A.M. Hardy, L. Gengembre, G. Leclercq, J. Catal. 117 (1989) 371.
[10] J.-M. Giraudon, L. Leclercq, G. Leclercq, A. Löfberg, A. Frennet, J. Mater. Sci. 28 (1993) 2449.
[11] T.R. Gengenbach, H.J. Griesser, Surf. Interf. Anal. 26 (1998) 498.
[12] D.J. Moon, M.J. Chung, M.K.Y. Park, S.I. Hong, Appl. Catal. A 168 (1998) 159.
[13] G.-L. Li, H. Nishiguchi, T. Ishihara, Y. Moro-oka, Y. Takita, Appl. Catal. B 16 (1998) 309.
[14] M.K. Neylon, S. Choi, H. Kwon, K.E. Curry, L.T. Thompson, Appl. Catal. A 168 (1999) 253.